

Comparative Study of Gallium Enhanced Microscopy and EBSD for Revealing Grain Boundaries and Dislocation Subgrain Boundaries in Aluminium Alloys

J. Hagström

Swedish Institute for Metals Research, Drottning Kristinas väg 48, 11428 Stockholm, Sweden

Keywords: Aluminium, Gallium, Grain boundaries, Dislocation boundaries, Liquid metal embrittlement, EBSD

Abstract

A new technique, gallium enhanced microscopy (GEM) for studying grain boundaries and dislocation subgrain boundaries in aluminium alloys was presented recently. By adding small amounts of gallium to aluminium alloys, increased visibility of grain boundaries and subgrain boundaries is achieved in the SEM. Recent GEM results show that boundaries with misorientations less than 1° can be detected due to the presence of gallium concentrated at them. The present paper describes briefly how the GEM method is applied and compares results obtained with this technique to characterisation using EBSD. Several comparative studies of a cold rolled AA3103 alloy annealed to different conditions were performed. The results show that GEM is a very reliable tool for the characterisation of grain boundaries as well as subgrain boundaries in aluminium alloys.

1. Introduction

Deformation substructure in aluminium alloys is sometimes difficult to characterise. Back-scatter electron (BSE) micrographs from the scanning electron microscope (SEM) do not give enough contrast to separate low angle subgrain boundaries and electron back-scatter diffraction (EBSD) has a limit in angular resolution of about 1.5° [1]. Gallium enhanced microscopy (GEM) is a recently developed technique for studying grain boundaries and subgrain boundaries in aluminium alloys [2, 3]. Recent GEM results where GEM and misorientation measurements in the transmission electron microscope (TEM) were compared showed that boundaries with misorientations of 1° or even less can be detected due to the presence of gallium concentrated at them [3]. Penetration of gallium along grain boundaries in aluminium is an example of the general phenomenon of liquid metal embrittlement and has been recognised for many years [4, 5]. The melting point of pure gallium is 30°C ; pure aluminium and gallium show an eutectic point at 97.9% Al and 26.6°C according to available phase diagrams [6]. Our experience was that this is lowered somewhat probably by the presence of iron and silicon so that, in commercial purity Al-alloys and Al-Mn-alloys, the phenomenon of liquid metal embrittlement occurs even at room temperature. Propagation of liquid Ga films along grain boundaries has been studied before, e.g. by TEM [7] and by synchrotron radiation microtomography [8]. The ability to separate grains in massive pieces of aluminium alloys from one another after exposure to Ga has been used to make metallographic studies of grain topography and also size distribution measurements in the past. The method was recently used also to show details of deformation structures and recrystallisation processes during aluminium sheet processing [2].

Other published results where gallium-decorated boundaries were studied with different methods indicate that low angle boundaries below 4° misorientation sometimes did not give any contrast. It has also been reported that special high angle boundaries with low energy were not recognised by X-ray synchrotron radiation. It appears, therefore, that atomic number BSE contrast in the SEM is more sensitive than other available techniques for this kind of study in aluminium alloys. Recent work on the softening behaviour of commercial AA1200 and AA3000 alloys using GEM show excellent agreement between microstructure evolution and modelled yield stress [9].

2. Experimental

The samples were prepared from AA3103 sheet that had been hot rolled to 4.2mm and cold rolled to 1.2mm by Hydro Germany.

Table 1: Alloy composition and main impurities, weight% (Optical Emission Spectroscopy) (Al bal.).

Mn	Fe	Si	Mg	Ti	Zn	Cu	Ni	B
1,04	0,54	0,07	0,009	0,006	0.005	0,003	0.002	0,001

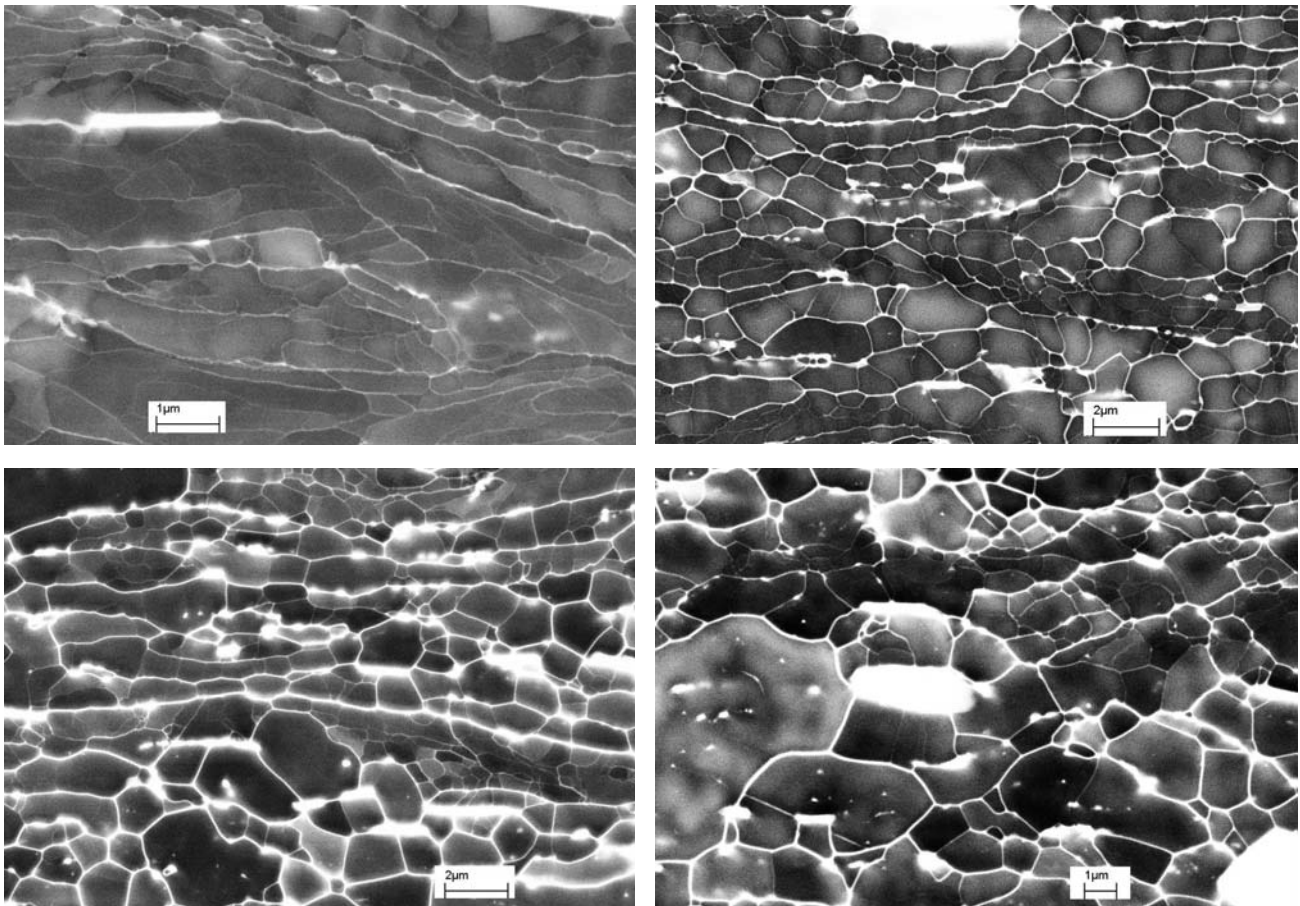
Back-annealing was carried out by Sapa Technology, the holding temperature was 290°C for the material presented in this paper. The heating rate was 50°C/h. Cooling from the annealing temperature was done in air. The conditions included in this investigation were; as cold rolled, 0h @ 290°C (heated to 290°C and then directly cooled), 2h @ 290°C, 6h @ 290°C, 12h @ 290°C, 24h @ 290°C, and 144h @ 290°C. The microstructural investigations were performed in the longitudinal section that contained the rolling and normal directions (RD-ND). Samples, 10mm*1.2mm*2mm, were mechanically polished using 3µm diamond paste in the final stage. The samples were then electro-polished to remove completely the mechanical deformations originating from polishing. The samples that were examined by EBSD were directly put in the microscope vacuum chamber and usually scanned over-night. Liquid gallium (with small amounts of Al, Mn, Fe, Si) was then applied on the opposite side to the electro-polished surface at room temperature and the specimens were directly put back in the SEM vacuum chamber. The gallium rapidly penetrates the grain boundaries and about 2h after application of gallium on the back-side of the sample the grain boundaries and subgrain boundaries at the electro-polished surface were decorated with gallium and thus possible to study with the microscope's BSE detector. The samples were analysed using a Leo Gemini field emission gun SEM (FEG-SEM) operating in BSE mode.

Recrystallised fractions were determined by applying a grid on GEM micrographs in low magnification (750X-1000X) and counting crosses in recrystallised and non-recrystallised areas. Since no information on misorientations was available in these images only grain size and morphology determined whether the grains were rated as recrystallised or not. Grain sizes and subgrain sizes were determined by applying the mean linear intercepts (MLI) method. Usually 10-15 micrographs were used for the determinations of recrystallised fraction and MLI for each material condition. The micrographs were spread over the surface and micrographs from several different depths from the sheet surface were always included.

3. Results

Examples of GEM micrographs in the cold rolled and back-annealed samples are shown in Figures 1-4. Results from recrystallised fraction evaluation and MLI measurements from the GEM micrographs are presented in Table 2. Figures 5 and 6 present examples of EBSD orientation maps. Table 3 gives details on the EBSD measurements.

GEM results - Both recrystallised fractions and small grain intercepts look consistent and show an expected trend (Table 2), i.e. increasing values with annealing time. The MLI length for large grains increase in the beginning for the vertical case, but are then rather constant from 12h annealing and longer. The average horizontal MLI length seems to be constant during the annealing according to these results. The largest grains were very large already in the 2h sample ($>80\mu\text{m}$ in the horizontal direction) and since new grains are evolving continuously the change of the average size of large grains ($>5\mu\text{m}$) is perhaps not very great. The microstructures were also very inhomogeneous with very large grains at about quarter depth and finer structure near the surface and in the middle.



Figures 1-4: GEM micrographs showing the evaluation of the non-recrystallised microstructure during back-annealing. Images come from the as cold rolled structure (1), from the 2 h back-annealed structure (2), from the 6 h back-annealed structure (3) and from the 24 h back-annealed structure (4).

EBSD results - It was previously known, and confirmed here, that EBSD results are very sensitive to step size and to the definition of boundaries (misorientation limits for grain boundaries and subgrain boundaries). It was difficult to analyse the microstructures because they were so very inhomogeneous. Subgrains range from fractions of microns to a few microns in size.

Recrystallised grains range from a few microns to one hundred microns in diameter. To characterise both recrystallised grains and deformed and recovered structures several EBSD maps with different step sizes were needed. The results in Table 3 with large variations in recrystallised fraction and grain size show that it is probably necessary to perform more measurements to achieve statistically sound values for the recrystallised fraction and for an evaluation of the recrystallised grain size.

Table 2: Recrystallised fraction and MLI as measured with GEM. The samples were heated from room temperature to the annealing temperature with a rate of 50°C/h.

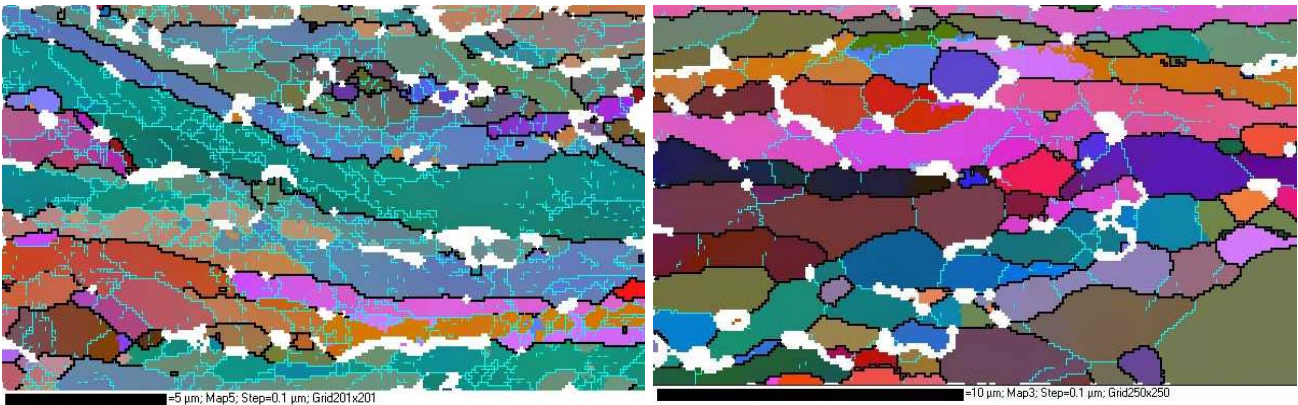
Ann. Temp. (°C)	Condition	Recrystal. fraction (%)	Large grain Intercepts (>5µm)			Small grain Intercepts		
			Horizontal (µm)	Vertical (µm)	Ratio (H/V)	Horizontal (µm)	Vertical (µm)	Ratio (H/V)
-	CR	0.0	-	-	-	0.76	0.32	2.4
290	0h	2.0	-	-	-	0.78	0.45	1.7
290	2	17.9	23.2	10.3	2.3	0.94	0.59	1.6
290	6	32.6	22.1	12.1	1.8	1.02	0.66	1.5
290	12	61.6	23.6	13.1	1.8	1.06	0.72	1.5
290	24	84.2	23.1	13.0	1.8	1.08	0.75	1.4
290	144	94.2	22.9	12.6	1.8	2.66	-	-

Table 3: Description of EBSD orientation maps and statistical data. In this table 1.5° misorientation was used as the lower limit for boundaries.

Ann. Temp. (°C)	Cond. (h)	Map			Grain Intercepts				Vertical Intercepts			Horizontal Intercepts		
		Dimension (steps)	Step (µm)	Hit Rate (%)	Recr. frac. (%)	Horizontal (µm)	Vertical (µm)	Ratio (H/V)	smallest (µm)	Largest (µm)	Ratio (H/V)	smallest (µm)	Largest (µm)	Ratio (H/V)
-	CR	201*201	0.1	61	-	0.69	0.47	1.5	0.1	2.2	0.05	0.1	5.3	0.02
-	CR	600*264	0.2	50	6	0.84	0.73	1.2	0.2	3.0	0.07	0.2	6.4	0.03
290	0	216*208	0.1	67	-	0.82	0.69	1.2	0.1	6.0	0.02	0.1	9.3	0.01
290	0	800*800	0.2	60	21	0.94	0.76	1.2	0.2	5.6	0.04	0.2	10.2	0.02
290	2	250*250	0.1	71	49	1.05	0.72	1.5	0.1	2.5	0.04	0.1	8.3	0.01
290	2	575*416	0.2	72	53	1.38	1.11	1.2	0.2	26.0	0.01	0.2	49.4	0.00
290	6	401*251	0.2	72	31	0.92	0.77	1.2	0.2	3.8	0.05	0.2	6.2	0.03
290	6	575*213	1	76	55	3.60	3.00	1.2	1.0	45.0	0.02	1.0	100.0	0.01
290	24	600*600	0.2	84	47	2.37	1.77	1.3	0.2	16.6	0.01	0.2	48.8	0.00

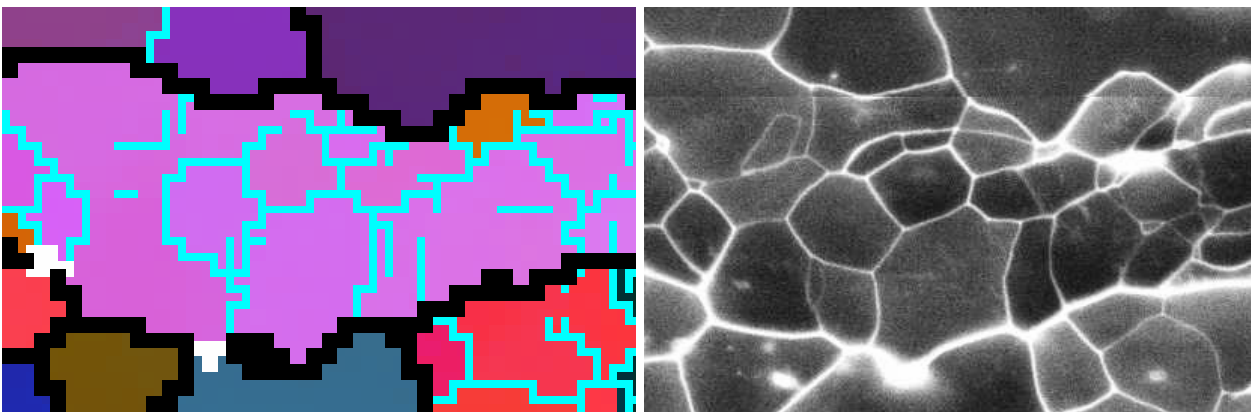
Table 4: MLI intercepts of the substructure in different conditions measured with EBSD.

Ann. Temp. (°C)	Cond. (h)	Map		2° misorientation		1.5° misorientation	
		Dimension (steps)	Step (µm)	Horizontal (µm)	Vertical (µm)	Horizontal (µm)	Vertical (µm)
-	CR	201*201	0.1	0.85	0.55	0.69	0.47
290	0	800*800	0.2	1.07	0.81	0.94	0.76
290	2	575*74	0.2	1.18	0.83	1.04	0.77
290	6	401*251	0.2	1.21	0.93	0.92	0.77
290	24	350*56	0.2	1.16	0.88	0.99	0.80

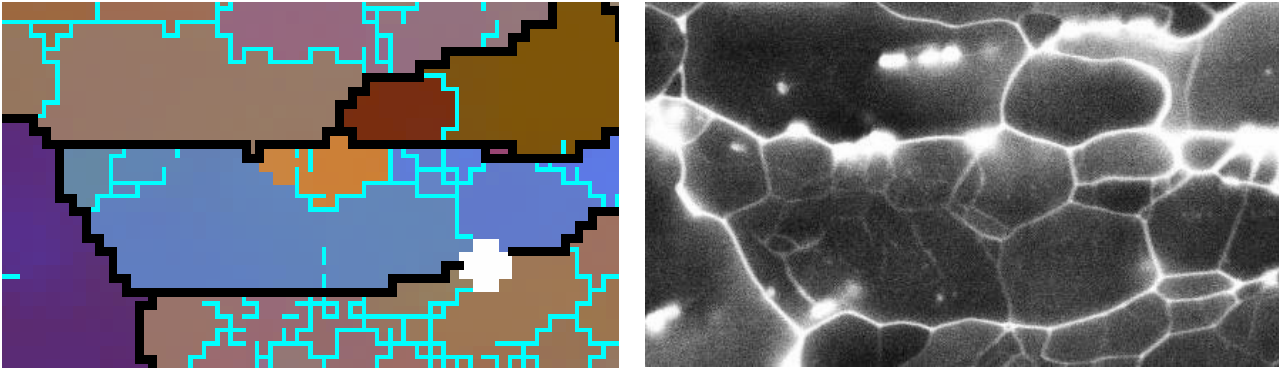


Figures 5, 6: EBSD orientation map from the as cold rolled material (5) and 2h annealed material (6). The hit rate was 61% and 71% in the respective maps. The maps were enhanced using “noise reduction” in the Tango software. The colours represent orientations according to the three Euler angles in “Euler space”, except the white colour which represent “zero solutions”, i.e. areas where the Kikuchi pattern could not be recognised. Black lines indicate grain boundaries with a misorientation larger than or equal 15° . Blue lines indicate grain boundaries and subgrain boundaries with smaller misorientations than 15° . The lower misorientation limit for boundaries is 1.5° in this figure.

Comparative study GEM vs. EBSD - GEM shows more details and finer (with lower misorientation) subgrain boundaries than EBSD does. This was shown for all conditions in this survey. Figures 7 and 8 a) b) show grains and subgrains characterised with both methods and it is clear that many of the boundaries that are present in the GEM micrographs have not been detected by EBSD. Table 5 compares MLI measurements from GEM micrographs and EBSD. The average MLI length from EBSD data is more than 50% larger than from GEM for the cold rolled material and the 0h annealed conditions, in the 24h annealed condition EBSD gives about 20% larger values. 2° misorientation was used as the lower limit for subgrains, this level was chosen because a lower limit creates many “one pixel subgrains” which is not in accordance with the real microstructure.



Figures 7 a, b: Comparison EBSD/GEM. a) EBSD orientation map from the 24h annealed material b) GEM micrograph of the same area as a).



Figures 8 a, b: Comparison EBSD/GEM. a) EBSD orientation map from the 24h annealed material b) GEM micrograph of the same area as a).

Table 5: MLI intercepts as measured with GEM and EBSD data.

Cond.	GEM		EBSD 2° misorientation	
	Horizontal (µm)	Vertical (µm)	Horizontal (µm)	Vertical (µm)
CR	0.76	0.32	0.85	0.55
0h	0.78	0.45	1.07	0.81
2	0.94	0.59	1.18	0.83
6	1.02	0.66	1.21	0.93
24	1.08	0.75	1.16	0.88

4. Conclusions

Gallium enhanced microscopy (GEM) micrographs give much more details on the microstructure than EBSD orientation maps. Many boundaries with low misorientation that are detected by GEM cannot be characterised with EBSD.

MLI measurements from EBSD data gave more than 50% larger subgrain sizes compared to similar measurements from GEM micrographs for the cold rolled material and the 0h annealed condition.

EBSD orientation maps on the other hand give more information than GEM micrographs since misorientation and texture information is available.

GEM easily covers large areas and micrographs can conveniently be spread out to obtain microstructural information on a statistically sound base. This is not easily achieved by EBSD.

The results presented in this report also show that it is difficult to give exact values of microstructural parameters. The resulting value is dependent on the evaluation parameter, the detection method, and, if manual methods are used, also on the operator.

5. Acknowledgements

This research was carried out with funding from the SIMR basic research program and from VIR[FAB] (Fifth Framework project, Contract N° G5RD-CT-1999-00132). The authors would like to thank the VIR[FAB] consortium for their collaboration and support. Funding

by the European Community is gratefully acknowledged. H-E. Ekström and O. Mishin at Sapa Technology and Prof. B. Hutchinson at SIMR are acknowledged for the material supply, the annealing trials and for valuable discussions and ideas during the development of the GEM method and the application of the method to characterise deformation substructures in aluminium alloys.

References

- [1] F.J. Humphreys, P.S. Bate and P.J. Hurley, *Journal of Microscopy*, 201, 50, 2001
- [2] J. Hagström and B. Hutchinson, *Materials Science Forum*, 396-402, 539, 2002
- [3] J. Hagström, O.V. Mishin and B. Hutchinson, Gallium enhanced microscopy for revealing grain boundaries and dislocation subboundaries in aluminium alloys, *Scripta Materialia*, 49, 1035-1040, 2003
- [4] W. Ludwig, S.F. Nielsen, H.F. Poulsen and D. Bellet, *Defect and Diffusion Forum*, 194-199, 1319, 2001
- [5] F.N. Rhines and B.R. Patterson, *Met. Trans. A*, 13A, 985, 1982
- [6] J.L. Murray, *BULL, ALLOY PHASE DIAGRAMS*, 183-190, 1983
- [7] Q. Liu. *Ultramicroscopy*, 60, 81, 1995
- [8] L. Ren, D.F. Bahr and R.G. Hoaglund, *Mat. Res. Soc. Symp. Proc.* 578, 411, 2000
- [9] H-E. Ekström, O Mishin and L. Östensson, Presented at this conference, 2004